Spatial and temporal nonlinearity of AutoResonant wakefield excitation

M. Luo[1], C. Riconda[2], A. Grassi[2], N. Wang[3], J. S. Wurtele[4], T. Fülöp[1], I. Pusztai[1]

[1] *Department of Physics, Chalmers University of Technology, Göteborg, Sweden*

[2] *LULI, Sorbonne Université, CNRS, École Polytechnique, CEA, 75252 Paris, France*

[3] *College of Electrical Engineering, Zhejiang University, Hangzhou 310027, China*

[4] *Department of Physics, University of California, Berkeley, California 94720, USA*

Autoresonant (AR) wakefield excitation has the advantage of being robust to plasma density and laser frequency uncertainties, while being able to generate a wakefield exceeding the Rosenbluth-Liu (RL) limit. We study the two nonlinear stages over the wakefield evolution and discussed the multiple-dimensional effects that impact the transverse structure of the wakefield.

We study multi-dimensional effects on the AR wakefield excited by two co-propagating laser with parallel linear polarization and identical intensities, using the particle-in-cell (PIC) code SMILEI [1]. The laser beams have a 6th-order super-Gaussian temporal profile $\propto \exp\left[-(t/T_{\rm pulse})^6\right]$, and transverse profile $\propto \exp\left[-(y/w_0)^6\right]$, where the laser width w_0 is $2.4\pi k_{\rm pe}^{-1}$. Here, $k_{\rm pe} = \omega_{\rm pe}/c$ is the inverse electron inertial length, with the electron plasma frequency $\omega_{\rm pe} = \sqrt{n_e e^2/\epsilon_0 m_e}$. The choice of the laser and plasma parameters were guided by our previous 1D study [2], to reach the wave-breaking limit. The laser amplitudes, in terms of the normalized vector potential $a = eA/m_e c$, are $a_1 = a_2 = 0.2$. The homogeneous plasma density is $n_e/n_{cr} = 0.0004$, with the critical density $n_{cr} = \omega_1^2 m_e \epsilon_0/e^2$ corresponding to the laser frequency ω_1. The first laser has a chirp rate α, leading to a frequency difference between the lasers $\Delta\omega = \omega_{\rm pe}[1+\alpha(t-t_0)\omega_{\rm pe}]$. At $t_0 = 22.5\pi/\omega_{\rm pe}$, this frequency difference matches the plasma frequency, $\Delta\omega = \omega_1 - \omega_2 = \omega_{\rm pe}$. The laser frequencies are $\omega_1/\omega_{\rm pe} = 50$ and $\omega_2/\omega_{\rm pe} = 49$, and the pulse duration $T_{\rm pulse}\omega_{\rm pe} = 64\pi$ is chosen to support AR growth of the wakefield until the wave-breaking limit. The ions are assumed immobile, as their dynamics is negligible on the timescale of the laser pulse [3]. More details of the simulation setup are given in [4].

Considering the computational expense of 2D studies, here we focused on the evolution of the process up to $t\omega_{\rm pe} \approx 750$. To highlight the impact of AR on the wakefield excitation, Fig. 1 shows the phase space $v_x - \xi$ (colormap), with the co-moving coordinate $\xi = \omega_{\rm pe}(x/c - t)$, and the longitudinal electric field E_L (red curve) of the wakefield at time $t\omega_{\rm pe} \approx 350$. Based on our recent study [4], at this time 2D effects have not yet impacted significantly the transverse coherence. In these figures, the phase space is obtained by averaging over the transverse direction $y \in [\pi, \pi]$ $(\pi < w_0)$, and the electric field is taken at the symmetry axis $y = 0$. Based on Newton's second law $dv_x/dt = -\frac{e}{m_e} e_L \sin(\theta)$ with e_L the wakefield amplitude, and the rapid oscillation

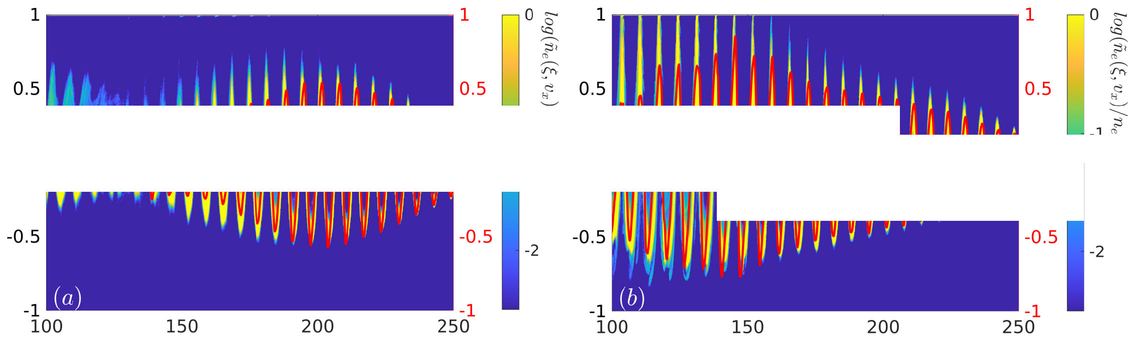

Figure 1: The phase space $v_x - \xi$ (colormap) and the longitudinal electric field (red curve) of the wakefield $\tilde{E}_L = e_L \sin(\theta + \pi/2)$ at the time instant of $t\omega_{\rm pe} \approx 350$, e_L is the wakefield amplitude. In (a), no chirp is applied, and in (b), the optimal chirp rate $\alpha = -0.0014$ is applied to the laser (1).

of the background electron plasma due to the electric force, the evolution of the phase space can be predicted by $v_x \sim \sin(\theta + \pi/2)$. Hence, Fig. 1 shows the profile of $\tilde{E}_L = e_L \sin(\theta + \pi/2)$ rather than $E_L = e_L \sin(\theta)$. Figures 1(a) and (b) both indicate that the oscillation in the phase space is a direct response of the plasma to the electric force. However, owing to the AR achieved by introducing an appropriate chirp of the first laser beam, the maximum wakefield strength in Fig .1(b) is stronger than that in Fig. 1(a) and particles gain relativistic velocity. Without chirp, the field saturates at the RL limit $E_{\rm RL}/E_0 \approx (16a_1a_2/3)^{1/3} = 0.6$, while in the AR case, the wave breaking limit amplitude is reached, $E_L \approx E_0 = m_e c\omega_{pe}/e$, and the self-injected electrons reach higher energies. Also, magnetic field perturbations are excited trough instabilities caused by perturbations of the density and flow velocity [5] and anisotropic heating [6], see the discussion in Ref. [4].

During AR, which is a weakly nonlinear phenomenon, the evolution of physical quantities at a given transverse position only depends on the coordinates along which the external parameter varies. This parameter is the frequency, which varies along ξ. Consequently, the wakefield and phase space profiles only depend on the coordinate ξ. We observed this quasi-1D behavior close to the symmetry axis for times $t\omega_{\rm pe} \leq 350$. However, 2D effects of wavefront bowing [7] and Raman scattering [8] inevitably happen, and they have an impact on the spatial structure of the wakefield in the transverse direction. To investigate this influence, we define the *structure function* of the wakefield in the transverse direction, i.e.,

$$C_L(\xi, l_s) = \frac{\int E_L(\xi, y - l_s/2) E_L(\xi, y + l_s/2) dy}{\int |E_L(\xi, y)|^2 dy}. \quad (1)$$

Here, the variations in this term can be understood by considering that the wakefield will be of